www.elsevier.com/locate/csr

Particle fluxes and recent sediment accumulation on the Aquitanian margin of Bay of Biscay

Sabine Schmidt, Hélène Howa, Aurelia Mouret, Fabien Lombard, Pierre Anschutz, Laurent Labeyrie

PII: S0278-4343(09)00023-5
DOI: doi:10.1016/j.csr.2008.11.018
Reference: CSR 1934

To appear in: *Continental Shelf Research*

Received date: 20 June 2008
Revised date: 30 September 2008
Accepted date: 20 November 2008

Cite this article as: Sabine Schmidt, Hélène Howa, Aurelia Mouret, Fabien Lombard, Pierre Anschutz and Laurent Labeyrie, Particle fluxes and recent sediment accumulation on the Aquitanian margin of Bay of Biscay, *Continental Shelf Research* (2009), doi:10.1016/j.csr.2008.11.018

Particle fluxes and recent sediment accumulation on the Aquitanian margin of Bay of Biscay

Sabine Schmidt[a,b,*], Hélène Howa[c], Aurelia Mouret[b], Fabien Lombard[d], Pierre Anschutz[b], and Laurent Labeyrie[d]

[a] CNRS, UMR5805 EPOC, F-33405 Talence Cedex, France

[b] Université de Bordeaux, UMR5805 EPOC, F-33405 Talence Cedex, France.

[c] University of Angers, UPRES EA 2644 BIAF, 2 Boulevard Lavoisier, 49045 Angers Cedex, France.

[d] UMR1578 LSCE, Avenue de la Terrasse, F-91198 Gif-sur-Yvette Cedex, France.

Corresponding author: Fax: + 33 (0)556 840 848; Tel: +33 (0)540 003 315; E-mail: s.schmidt@epoc.u-bordeaux1.fr

Abstract

As a part of the ANR-Forclim experiment, particle mass fluxes and sedimentation processes were investigated on the slope of Aquitanian margin of the Bay of Biscay, between the canyons of Cap Breton and Cap Ferret. Interface sediments were collected along a depth transect from 145 m to 2000 m; simultaneously a mooring line was deployed at the deepest station (WH, 2000 m) with two traps (800 m and 1700 m) for a 16-month period (June-2006 – November 2007). ^{210}Pb activities of settling particles and of interface sediments were determined to study transport processes of particles. Sediment and mass accumulation rates, calculated from excess ^{210}Pb profiles in the sediment column, show the expected decreasing trend with depth, as usually observed on margins. Mean particulate mass fluxes at 800 m and 1700 m depth at site WH are respectively 27 and 70 g m^{-2} a^{-1}.

The ^{210}Pb budget points out events of temporary high lateral input of particles. The comparison of mass and ^{210}Pb fluxes between the water column and the seabed indicates that lateral transport plays an important role in particle accumulation on the Aquitanian margin. Regarding the objectives of the ANR-Forclim program, which aims to improve significantly the interpretation of fossil foraminifera signals, as a proxy for hydrological changes in the North Atlantic ocean, these results highlight advection processes must be considered when interpreting fluxes of foraminifers on the Aquitanian margin.

Keywords

Bay of Biscay, Aquitanian margin, particulate mass flux, ^{210}Pb activity and flux

Introduction

The present work is a contribution to the ANR-Forclim program; main objective is to improve significantly the interpretation of fossil foraminifera signals, as a proxy for hydrological changes in the North Atlantic ocean. The export of foraminifera shells is usually assumed to be fully transferred into the sediment, and through their species assemblage, to provide a sedimentary record of past seasonal productivity conditions of the upper ocean (Lončarić et al., 2007). Nonetheless, like all organisms, the community structure of planktic foraminifera is largely influenced by their surrounding environment (Bàrcena et al., 2004; Retailleau et al., submitted). The distribution of microfossils in surface sediment could differ from the biogenic assemblages recorded in the sediment traps in relation with different factors like differences in time scales, since surface sediments represent an integrated signal of several decades to centuries, dissolution processes or lateral advection (Bàrcena et al., 2004). Therefore, a preliminary task of the ANR-Forclim program was to characterize the sedimentary environment of foraminifera growth in the water column and at the water-sediment interface in order to explain potential discrepancies between trap and seabed records.

The experiment area is the Aquitanian margin, in the south-eastern part of the Bay of Biscay. The Aquitanian margin is bordered by two large canyons (Cap Ferret Canyon, Cap Breton Canyon, Fig. 1). The hydrographical structure is relatively well known (Ogawa and Tauzin, 1973). The patterns of the surface waters are strongly constrained by seasonal variations of the thermocline and of the mixed layer. Well characterized by its high salinity, Mediterranean Outflow Waters are present between 600 and 1300 m. Several rivers in France and Spain (Loire, Charente, Gironde, Adour, Bidassoa, and Nervion) feed the sedimentary basin of the Bay of Biscay; the Gironde and Loire Rivers are presently the main sources of fine sediments to the margin (Castaing et al., 1999; Jouanneau et al., 1998). Sediments on the slope consist of mud composed of clay, silt, and of less than 30% carbonates (Hyacinthe et al., 2001). Primary production in the Bay of Biscay is less documented: during ECOFER experiment, in the Cap Ferret Canyon, primary production presented seasonal variability from 0.7 - 1.2 g C m^{-2} d^{-1} in spring (May 1990 and 1991) to 0.3 g C m^{-2} d^{-1} in autumn (October 1990), with an annual primary production of about 145 - 170 g C m^{-2} a^{-1} (Laborde et al., 1999). In the last two decades, several projects have focused on continental margins in order to understand particle dispersion, for the North Atlantic: SEEP on the outer margin of the Mid Atlantic Bight (Biscaye and Anderson, 1994), ECOFER in the Cap Ferret canyon (Heussner

et al., 1999), OMEX in the northern Bay of Biscay and on the north-western Iberian margin (van Weering et al., 1998; 2002) or ENAM on the European North Atlantic Margin (Mienert, 1998). The occurrence of the two large canyons on both sides, where occurs efficiency particle transfer (Heussner et al., 1999; Durrieu de Madron et al., 1999) had seem to detract the interest in particle transfer on the Aquitanian margin, except few investigations on early diagenesis processes in sediment (Chaillou et al., 2002; Hyacinthe et al., 2002) and on living benthic foraminifera faunas in relation with organic matter flux (Fontanier et al., 2002).

Lead-210 (^{210}Pb) is a naturally occurring radionuclide in marine sediments, and has been widely used to study sediment dispersal and accumulation on century timescales (Cochran, 1992). Particles, organic or inorganic, scavenge ^{210}Pb from the water column and deposit at seabed ^{210}Pb in excess ($^{210}Pb_{xs}$) of that produced within sediments by the decay of its parent isotope, ^{226}Ra. As sediments are buried, ^{210}Pb decays with its half-life of 22.3 years. From profiles of $^{210}Pb_{xs}$ with depth in sediment, it is therefore possible to calculate sediment and mass accumulation rates on a decennial to secular time scale. The comparison of ^{210}Pb fluxes to its known production rate provides additional information on particle transfer throughout the water column (Biscaye and Anderson, 1994; Legeleux et al., 1996; Radakovitch et al., 1999, van Weering et al., 1992).

This work presents particulate mass and ^{210}Pb fluxes determined from two time-series sediment traps deployed at the main ANR-FORCLIM site (WH) and from interface cores taken along a depth transect (D, B, A, WH) on the Aquitanian margin of the Bay of Biscay. The ^{210}Pb budget between the water column and the seabed had offered the possibility to quantify the contribution of lateral input of sediment to the total particulate mass flux. Regarding the objectives of the ANR-FORCLIM program, the main objective of our work has been to estimate if sediment trap record of particulate mass fluxes at the site WH is representative of the deposition at the water-sediment interface.

2. Materials and methods

2.1. Interface sediment sampling

During the cruises PECH1 (June, 21-27, 2006) and PECH5 (Mars, 1-9, 2008), interface sediments were collected using a multicorer along a depth transect between 140 and 2000 m water depth (Fig. 1). The four stations D, B, A, and WH have been selected to compose a rather ideal SE-NW transect, ranging from the outer shelf to mesobathyal open slope environments (Fig. 1; Table 1). Above 700 m, the sediments of stations D and B are in contact with North Atlantic Central Waters, whereas site A and WH are under the influence of the

vein of Mediterranean waters. The bottom of the station WH is overlaid by North Atlantic Deep Waters. Immediately after core retrieval, tubes were carefully extruded with sediment taken at 0.5 cm interval from 0 to 2 cm, and 1 cm interval below. The samples were frozen and brought back to the laboratory for analysis.

2.2. Sediment trap sampling

During the cruise PECH1, a long-term mooring with two sediment traps (PPS5 TECHNICAP; sampling area 1 m^2) was deployed at the deepest station, WH, on the Plateau des Landes (Fig. 1, 44°33N, 2°43W, 2000 m water depth). Settling particles were sampled at two depths, 800 m and 1700 m respectively. The mooring was recovered in April and November 2007 during cruises PECH3 (April, 14-17, 2007) and PECH4 (November, 23-30, 2007). Sampling periods were 22 June 2006 to 6 April 2007, and 16 April to 23 November 2007, with variable sampling intervals (5-12 days). Unfortunately, due to a technical problem, the collection at 800 m stopped after 20 July 2007 during the second mooring period. The 24 collecting cups were filled with filtered seawater previously collected at depth, filtered on 0.45 μm pore size filter and poisoned with NaN_3. After recovery, the samples were stored in a refrigerator.

During the cruise PECH4 (November, 23-30, 2007), seawater for Ra determination was collected at selected water depths from the CTD-cast. This water was acidified and stored in dark 20-l bottles.

2.3. Analytical procedures

Back to the laboratory, to check the preservation of trapped particles, an aliquot of the supernatant was sampled for analyses of dissolved inorganic nitrogen (DIN) and phosphorus (DIP) content, to compare with the initial filling water. Trap samples were splitted into half aliquots using a rotating wet-sample divider (Lončarić et al., 2007). One half was used to determine mass fluxes. Particles were recovered by centrifugation, rinsed with deionised water to remove salts, lyophilized and weighted to estimate particle mass. Thereafter this fraction was used to measure ^{210}Pb and ^{226}Ra by gamma spectrometry (Schmidt et al., 2007). The detector is a low background, high-efficiency, well-shaped-detector (Canberra, Ge volume 280 cm^3), placed in a lead shield and protected from cosmic ray muons using an anti-cosmic shielding made of plastic scintillators. ^{210}Pb was determined by its specific ray at 46.5 keV, and ^{226}Ra by the rays of its decay products, at 295 and 352 keV for ^{214}Pb and 609 keV for ^{214}Bi. Standards used for the calibration of the γ detector were IAEA standards (RGU-1,

RGTh-1). The counting error was one standard deviation of counting, and counting times were from 4 to 24 hours. Excess ^{210}Pb in settling particles, $^{210}Pb_{xs}$, i.e. that scavenged from seawater, was calculated by subtracting the activity supported by its parent isotope, ^{226}Ra, from the total ^{210}Pb activity in the sediment. Isotopes of the ^{238}U-decay series were assumed to be in secular equilibrium in the detritical phases. In all trap samples $^{210}Pb_{xs}$ represents 92 - 99 % of the total ^{210}Pb in the particulate matter. Error on $^{210}Pb_{xs}$ was calculating by propagating errors on ^{210}Pb and ^{226}Ra determinations. Radium was co-precipitated with $BaSO_4$ from the seawater and radium activities were measured by γ-counting (Schmidt and Reyss, 1996). Particulate organic carbon was measured on freeze-dried samples by infrared spectroscopy using a LECO C-S 125, after removal of carbonates with 2M HCl from 50 mg of powdered sample.

Supernatant DIP concentrations were measured using the molybdate blue method of Murphy and Riley (1962). Supernatant DIN consisted of dissolved nitrate+nitrite and ammonia. Nitrate+nitrite were measured by flow injection analysis (FIA) according to Anderson (1979). Ammonium was analyzed with the colorimetric method described by Aminot and Chaussepied (1982).

Sediment samples were dried at 60°C,. Dry bulk density (DBD) was calculated by comparing the weight of wet and dry sediment (Schulz and Zabel, 2006). Following this procedure, sediment samples were crushed and stored in sealed plastic tubes; ^{210}Pb and ^{226}Ra activities were measured and $^{210}Pb_{xs}$ calculated as described previously.

3. Results

3.1. Interface sediment

Excess ^{210}Pb and DBD are presented versus depth from top cores (Figure 2). DBD profiles were quite similar at each station, showing the expected increase with depth, due to the compaction of sediment and the associated decrease in water content. Sites A and B were sampled two times, in June-06 and April-08: profiles of DBD were quite similar.

Along the depth transect, surface excess ^{210}Pb activities ranged from 16 to 55 dpm g^{-1} (Figure 2), increasing with depth. Profiles of $^{210}Pb_{xs}$ presented large differences depending on the core location. On the shelf (site D), $^{210}Pb_{xs}$ exhibited moderate and almost constant activities throughout the core. On the upper slope (site B), a weak mixed layer was noticeable in the upper 2-3 cm of the $^{210}Pb_{xs}$ profile, followed by a penetration at a depth deeper to 10 cm. On the middle slope (sites A and WH), ^{210}Pb activities decreased exponentially; reaching supported activity levels at about 5-8 cm depth. With no evidence of strong disturbance

(except for core A-06), such a feature is appropriate to the determination of sediment accumulation rates.

3.2. Trapped particulate fluxes

The total particulate mass flux, registered by the sediment traps moored at site WH, varied between 16 and 362 mg m^{-2} d^{-1} at 800-m depth and between 34 and 812 mg m^{-2} d^{-1} at 1700-m depth (Figure 3). During the experiment, mean trapped particulate fluxes were 75 and 192 mg m^{-2} d^{-1} (27 and 70 g m^{-2} a^{-1}) at 800-m and 1700-m depth. Particle flux was much higher at the depth of the deeper trap. In addition, the deeper trap recorded the wider range and variability, with large and abrupt mass flux variations, especially in winter and early spring. In December 2006 and February 2007, flux at 1700 m peaked at 812 and 620 mg m^{-2} d^{-1}. This indicates that large total mass flux variations could take place rapidly for a short period.

$^{210}Pb_{xs}$ specific activities of settling particles ranged between 110 and 267 dpm g^{-1}, with higher levels and variability in the deeper trap (Figure 4). These values are in the range of already published data for margin at equivalent depths (Biscaye and Anderson, 1994; Legeleux et al., 1996; Chung et al., 2004; Radakovitch et al., 1999): $^{210}Pb_{xs}$ showed a general tendency to increase with depth. Specific activities revealed significant variations associated with changes in mass fluxes, the lowest activities were usually associated with the highest mass fluxes (Figure 4), as already reported on margin (Legeleux et al., 1996). $^{210}Pb_{xs}$ fluxes were mainly influenced by total mass fluxes (Figure 4).

Organic carbon ranged between 3.7 and 17.3 % at 800-m depth and between 3.2 and 10.2 % at 1700-m depth (Figure 5). Enrichment of DIP and DIN in supernatant indicated that, despite poisoning, a minor part of particulate organic carbon was mineralized *in situ* within trap sampling vials after their closure. A correction was made, using DIN and a Redfield ratio for organic matter, to estimate the proportion organic carbon that was consumed. This proportion was generally below 20% of the measured organic carbon, as reported in Fig. 4. Therefore, the loss of mass due to mireralization did not affect significantly the total particulate mass flux. There was a clear decrease in organic carbon content of settling particles with depth that could be ascribed to particle mineralization during their settling throughout the water column and to the advection of low-carbon particles. In the deepest trap, the highest mass fluxes were always associated with the lowest carbon content (Figure 5).

^{226}Ra activities in the water column ranged between 7.9 and 11 dpm l^{-1}, the highest levels were observed at 1700 m, due to Ra diffusion from sediment (this effect is more pronounced

for ^{228}Ra). These values are in the range of published data for the North-East Atlantic (Schmidt, 2006). This profile was used to estimate the ^{210}Pb production rate by the decay of ^{226}Ra in the water column above the sampling sites (Table 2).

4. Discussion

4.1. Sedimentation ad mass accumulation rates

The ^{210}Pb method is based on the measurement of the excess or unsupported activity of ^{210}Pb (^{210}Pb$_{xs}$) which is incorporated rapidly into the sediment from atmospheric fallout and water column scavenging (Appleby and Oldfield, 1992; and references herein). Once incorporated into the sediment, unsupported ^{210}Pb decays with depth, equivalent to time, in the sediment column according to its known half-live. By applying this principle, it is assumed that the specific activity of newly-deposited particles at a given site is constant with time. Therefore, sediment accumulation rate can be derived from ^{210}Pb, based on two assumptions: constant flux and constant sediment accumulation rate (referred to as the CF:CS method) (Robbins et al., 1975). Then, the decrease of ^{210}Pb$_{xs}$ activities with depth is described by the following relation:

$$\left[^{210}\mathrm{P}b_{xs}\right]_z = \left[^{210}\mathrm{Pb}_0\right]_0 \exp(-z\frac{\lambda}{S}) \qquad (1)$$

where $[^{210}Pb_{xs}]_{0,\,z}$ are the activities of excess ^{210}Pb at surface, or the base of the mixed layer, and depth z, λ the decay constant of the nuclide, and S the sediment accumulation rate. In this model, the compaction effect is not considered, and these sediment accumulation rates correspond to maximum values. An alternative method is to plot the regression of ^{210}Pb$_{xs}$ against cumulative mass to calculate a mass sedimentation rate (MAR), which integers compaction effect. Both estimates are given, as the first one is the mostly used (Table 1). Estimates for core D need to be considered with caution; indeed ^{210}Pb$_{xs}$ profiles of core D presents a weak decrease with depth, which could be ascribed to recent high deposition rates or to mixing event. This core serves only as an indication that high deposition rate occurs on the shelf.

Sedimentation and mass accumulation rates show decreasing values with depth, as usually observed in margin and canyon sediments (Sanchez-Cabeza et al., 1999; van Weering et al., 2002; Muhammad et al., 2008). MAR agree with previous estimates on cores collected 8 years ago on the Aquitanian margin (Hyacinthe et al., 2002). Sedimentation rates on the upper slope of the Aquitanian margin are higher, at equivalent depths, than those observed at

Goban Spur and Meriadzek on the northern margin of the Bay Biscay (van Weering et al., 1998). However values are lower to those obtained in the Cap-Ferret canyon on the northern border of the Aquitanian margin (Radakovitch et al., 1999). In fact, at about 500 m, SAR in the canyon and on the margin are in the same range (about 100 – 250 mg cm^{-2} a^{-1}). Then, the difference increases between these two nearby systems: at about 2000 m, SAR is 28 mg cm^{-2} a^{-1} at site WH, compared to 160 mg cm^{-2} a^{-1} in the Cap-Ferret canyon axis. The high values reported for the canyon are not surprising as canyons are usually presented as natural conducts for particle transfer to the deep ocean (Schmidt et al, 2001). By comparison with the above canyon system, the slope of the Aquitanian margin appears as a system where significant particle dynamics occur, but less efficient in particle transfer to deep ocean.

4.2. Excess ^{210}Pb inventory and focusing ratio

The effects of bioturbation or sediment advection could introduce some uncertainties in sedimentation rates derived from $^{210}Pb_{xs}$ excess. An alternative way to estimate deposition fluxes is to use $^{210}Pb_{xs}$ inventories, as bioturbation mainly affects the profile of $^{210}Pb_{xs}$ within the sediment. The seabed inventory of $^{210}Pb_{xs}$ is calculated (I, dpm cm^{-2}) as:

$$I = \Sigma A_i \, DBD_i \, dz$$

Where A_i is the excess ^{210}Pb of the sampled layer i, dz (cm) and DBD_i (g cm^{-3}) are respectively the thickness (0.5, 1, or 2 cm) and the dry bulk density of this layer. For site D, sediment $^{210}Pb_{xs}$ inventory is only a minimum value as $^{210}Pb_{xs}$ still presents high excesses at the base of the core (Figure 2). From this inventory, it is possible to calculate the annual $^{210}Pb_{xs}$ flux (dpm cm^{-2} a^{-1}) required to support the observed inventory at steady state (Biscaye and Anderson, 1994), as:

$$F = \lambda I$$

It is also interesting to compare this annual seabed $^{210}Pb_{xs}$ flux (F) and the predicted ^{210}Pb flux (P) using the focusing ratio (F/P). In the open ocean, the sources of ^{210}Pb are atmospheric fallout of ^{210}Pb to surface waters and its production in the water column from decay of ^{226}Ra (Cochran et al, 1990). For atmospheric deposition, we use the value of 0.51 ± 0.08 dpm cm^{-2} a^{-1} (Cochran et al., 1990); the production rate from the water column was calculated using the profile of ^{226}Ra at site WH (Table 2). Values of F/P > 1 suggest focusing or lateral input of ^{210}Pb to the considered site (Muhammad et al., 2008).

The highest values of F/P occur along the upper slope, where F/P ratios are higher to 8 for sites D and B. These high F/P ratios reveal high enrichments of seabed $^{210}Pb_{xs}$ flux with

respect to vertical scavenging of *in situ* production. On the middle slope (sites A and WH), the intermediate values of F/P (1.2 – 2.1) suggest a decrease of the lateral input; this observation is consistent with the decrease in sediment accumulation rate.

4.3. Particulate and ^{210}Pb fluxes in the water column

Mean mass fluxes at 800 m and 1700 m depths at site WH are respectively 27 and 70 g m^{-2} y^{-1} (Table 1) which are in the upper range of the values reported at equivalent depths over the Goban Spur and Meriadzek Terrace at the northern margin of the Bay of Biscay (47–50°N, 16-91 g m^{-2} yr^{-1}) (van Weering et al., 1998) and over the north-western Iberian Margin (41–44°N, 30-50 g m^{-2} yr^{-1}) (Schmidt et al., 2002). During the experiment, there was an obvious increase in mass fluxes between the deepest trap (300 m above bottom) and the seabed.

If sediment traps reliably record the particulate mass flux through the water column, mean annual trapped fluxes of $^{210}Pb_{xs}$ should be equivalent to the long-term rate of supply required to maintain $^{210}Pb_{xs}$ inventories in sediment. Table 2 compares the mean trapped ^{210}Pb fluxes, as recorded from June 2006 to November 2007 at 800 and 1700 m depths, to the flux recorded in the underlying sediment. At 800 m, the mean annual ^{210}Pb flux is much lower than seabed ^{210}Pb flux. The discrepancy results mainly by the fact that this trap was deployed more than 1000 m above the bottom. ^{210}Pb scavenging occurs throughout the water column (Cochran, 1992), leading to an increase of specific activities and fluxes between the two traps. Sediment resuspension could also contribute to the increase in ^{210}Pb fluxes. At 1700 m, only 300 m above bottom, the mean settling ^{210}Pb flux agrees rather well with the recorded inventories in the sediment (Table 2).

This good agreement tends to indicate that particulate fluxes recorded in the observed period are representative of longer term accumulation period.

4.4. F/P ratios of trapped particles

Mean F/P ratios of trapped particles increase with depth from 0.7 at 800 m to 1.2 at 1700 m (Table 2), indicating an increase of the contribution of lateral input toward seabed. As for $^{210}Pb_{xs}$ fluxes, mean F/P of trapped particles agrees with the recorded F/P in the underlying sediment, supporting the representativeness of sediment trap fluxes compared to interface sediments.

Legeleux et al. (1996) reported F/P ratios of trapped particles of about 0.5-1 at a mesotrophic site on the tropical N-E Atlantic margin, and concluded that eastern margins of

the tropical Atlantic, like margins of the Eastern Pacific (Moore et al., 1981; Carpenter et al.; 1981; Cochran et al., 1990) are significant sink for ^{210}Pb. F/P ratios of trapped particles and of sediments measured during the present work show that sediments of the Aquitanian margin may play also a role in the ^{210}Pb oceanic budget of the North-Atlantic, as they accumulate more ^{210}Pb than produced in the water.

The interest of trapped particles, compared to seabed inventories, is to document also short-time scale changes of $^{210}Pb_{xs}$ fluxes and therefore of F/P ratios. In fact the aforementioned mean F/P ratios conceal large variations in F/P ratios of trapped particles: from 0.2 to 3 at 800 m and from 0.2 to 4.1 at 1700 m (Table 2). This indicates drastic changes in the contribution of lateral input to the settling particulate fluxes throughout the year. It is noticeable that the highest F/P ratios are associated with low carbon organic particles (Figure 5). Time-series of mass flux and of F/P seem to indicate the occurrence of high flux events which are likely in relation with episodic near-bottom lateral transport of resuspended particles. These events are more frequent in autumn and in winter when temporary high mass fluxes are recorded (Figure 2), and affect mainly the deepest trap. The upper trap, at 1200 m above bottom, is less influenced by such lateral inputs.

In the absence of physical survey, sea surface temperature (SST) is used as a rough estimate of hydrodynamic conditions (Figure 3). SST of WH area shows temporal variations in agreement with season, the highest temperatures being recorded end summer. Superimposed on this general trend, abrupt decreases are visible that we could ascribe to mixing events of surface waters and the subsequent temperature decreases. Such events may record periods of high dynamics in the considered area. We can observe that the highest fluxes occurred almost simultaneously to such events. This could be an indication that the intensity of lateral input is controlled by the hydrodynamic.

4.5. Processes of lateral transport

Despite a gradual decrease of mass accumulation rates along the slope of the Aquitanian margin (Table 1), particle deposition on mid-slope is still high compared to the mean particle fluxes recorded in the deeper trap. Such high deposition rates have been already reported for the southern Middle Atlantic Bight or the Ikinanawa Trough for example (Biscaye and Anderson, 1994; Oguri et al., 2003), where lateral transport plays an important role in particle accumulation. The ^{210}Pb budget, as determined by the ratio of measured fluxes to the rate of ^{210}Pb production in the water column above the trap, implies temporary high lateral input, as observed in the Cap-Ferret canyon (Radakovitch et al., 1999). Rivers and coastal runoff

discharge large quantities of suspended particulate matter onto the continental shelf of the Bay of Biscay (Ruch et al., 1993; Castaing et al., 1999; Dubrulle et al., 2007; Jouanneau et al., 2008), with subsequent dispersion of suspended particles through shelf-slope exchange (Durrieu de Madron et al., 1999). The ECOFER study well established the role of the Cap-Ferret canyon as an active pathway of shelf-slope exchange of SPM for the Bay of Biscay (Heussner et al., 1999 Radakovitch et al, 1999). The present investigation indicates that the upper slope of the Aquitanian margin is also active in particle dispersion.

Regarding the sources of advected particles and the currents responsible for this transport, there were no systematic hydrographic surveys of the Aquitanian margin during the ANR-Forclim cruises and, therefore, no general picture of the water masses distribution and of the dispersion of the SPM during the mooring experiment. However, from the ECOFER program, a particle transfer scenario was proposed for the Cap-Ferret canyon margin, northward the Plateau des Landes (Figure 1) (Heussner et al., 1999). The slope circulation, characterized by a northward along-slope current with occasional reversals, and seasonal eddy activity were proven to be important mechanisms that control the entrainment and the dispersion of SPM on the Aquitanian margin (Durrieu de Madron et al., 1999). Durrieu de Madron et al. (1999) calculated that, resuspension of upper slope sediments (> 1000 m), through internal tides for example, is possible on the Aquitanian margin. This scenario gives an important role to resuspension processes and is consistent with the present high F/P ratios and low carbon organic particles recorded during the high particulate mass flux events on the Plateau des Landes.

Conclusions

Present-day sedimentation on the Aquitanian margin was assessed using ^{210}Pb and particulate mass fluxes along a depth transect. Sedimentation intensity (particulate fluxes, mass accumulation rates, ^{210}Pb budget) supports the occurrence of significant advection of sediments, even at the deepest site. Although such mass transfer affects mostly fine particle fraction, Brunner and Biscaye (2003) report events of resuspension and transport of foraminifera on the Southern Middle Atlantic. For this reason, these advection processes will be considered when interpreting sediment trap faunas and interface sediment assemblages of the ANR-FORCLIM program.

Besides, sediment trap and core-top ^{210}Pb fluxes were compared to determine whether the sediments have been altered since deposition. The mean settling ^{210}Pb fluxes at 300 m above

bottom agreed rather well with the recorded seabed ^{210}Pb inventories, indicating particulate fluxes recorded in the observed period were representative of longer term accumulation period. Therefore the ^{210}Pb budget supports the comparison of the sediment traps and nearby core-top assemblages in this study.

Acknowledgments

Crews of the R/V "Côte de la Manche" (CNRS-INSU), engineers of Technical Department INSU are gratefully acknowledged for their help with sampling. This study is financially supported by the ANR (Agence Nationale de la Recherche, France) to FORCLIM, by the ACI Jeunes Chercheurs ARTTE, and by the Regional Council of Aquitaine.

References

Aminot, A., Chaussepied, M., 1982. Manuel des analyses chimiques en milieu marin. Publication CNEXO, Brest, pp 390.

Anderson, L., 1979. Simultaneous spectrophotometric determination of nitrite and nitrate by flow injection analysis. Analitica Chimica Acta 110, 123-128.

Appleby, P. G., Oldfield, F., 1992. Application of lead-210 to sedimentation studies. Ivanovich, M., and Harmon, R., eds, Uranium Series Disequilibrium-Application to Environmental Problems: Applications to Earth, Marine, and Environmental Sciences, 2nd Edition, Oxford Press, London, pp. 731-778.

Bárcena, M.A., Flores, J.A., Sierro, F.J., Pérez-Folgado, M., Fabres, J., Calafat, A., Canals, M., 2004. Planktonic response to main oceanographic changes in the Alboran Sea (Western Mediterranean) as documented in sediment traps and surface sediments. Marine Micropaleontology 53, 423-445.

Biscaye, P.E., Anderson, R.F., 1994. Fluxes of particulate matter on the slope of the southern Middle Atlantic Bight: SEEP-II. Deep-Sea Research II 41, 459–509.

Brunner, C.A., Biscaye, P.E., 2003. Production and resuspension of planktonic foraminifers at the shelf break of the Southern Middle Atlantic Bight. Deep Sea Research I 50, 247-268.

Carpenter, R., Bennett, J.T., Peterson, M.L., 1981. ^{210}Pb activities in and fluxes to the Washington continental slope and shelf. Geochimica et Cosmochimica Acta 45, 1155-l 172.

Castaing, P., Froidefond, J. M., Lazure, P., Weber, O., Prud'homme, R., Jouanneau, J. M., 1999. Relationship between hydrology and seasonal distribution of suspended sediments on the continental shelf of the Bay of Biscay. Deep Sea Research II 46, 1979-2001.

Chaillou, G., Anschutz, P., Lavaux, G., Schäfer, J., Blanc, G., 2002. The distribution of U, Mo, and Cd in modern marine sediments. Marine Chemistry 80, 41-59.

Chung, Y., Chang, H.C., Hung, G.W., 2004. Particulate flux and ^{210}Pb determined on the sediment trap and core samples from the northern South China Sea. Continental Shelf Research 24, 673-691.

Cochran, J. K, 1992. The Oceanic Chemistry of the Uranium and Thorium-Series Nuclides. Ivanovich, M., and Harmon, R., eds, Uranium Series Disequilibrium-Application to Environmental Problems: Applications to Earth, Marine, and Environmental Sciences, 2nd Edition, Oxford Press, London, pp. 334-395.

Cochran, J.K., McKibbin-Vaughan, T., Dornblaser, M.M., Hirschberg, D., Livingston, H.D. Buesseler, K.O., 1990. ^{210}Pb scavenging in the North Atlantic and North Pacific Oceans. Earth and Planetary Science Letters 97, 332-352.

Dubrulle, C., Jouanneau, J.M., Lesueur, P., Bourillet, J.F., Weber, O., 2007. Nature and rates of fine-sedimentation on a mid-shelf: "La Grande Vasière" (Bay of Biscay, France). Continental Shelf Research 27, 2099-2115.

Durrieu de Madron, X., Castaing, P., Nyffeler, F., Courp, Th., 1999. Slope transport of suspended particulate matter on the Aquitanian margin of the Bay of Biscay. Deep-Sea Research II 46, 2003-2027.

Fontanier, C., Jorissen, F. J., Licari, L., Alexandre, A., Anschutz, P., Carbonel, P., 2002. Living benthic foraminiferal faunas from the Bay of Biscay: Faunal density, composition, and microhabitats. Deep-Sea Research I 49, 751-785.

Heussner, S., Durrieu de Madron, X., Radakovitch, O., Beaufort, L., Biscaye, P.E., Carbonne, J., Delsaut, N., Etcheber, H., Monaco, A., 1999. Spatial and temporal patterns of downward particle fluxes on the continental slope of the Bay of Biscay (northeastern Atlantic). Deep-Sea Research II 46, 2101-2146.

Hyacinthe, C., Anschutz, P., Carbonel, P., Jouanneau, J.-M., Jorissen, F. J., 2001. Early diagenetic processes in the muddy sediments of the bay of biscay. Marine Geology 177, 111-128.

Jouanneau, J.-M., Weber, O., Grousset, F.E., Thomas, B., 1998. Pb, Zn, Cs, Sc and Rare Earth Elements as Tracers of the Loire and Gironde Particles on the Biscay Shelf (Sw France). Oceanologica Acta 21, 233-241.

Jouanneau, J.-M., Weber, O., Champilou, N., Cirac, P., Muxika, I., Borja, A., Pascual, A., Rodríguez-Lázaro, J., Donard, O., 2008. Recent sedimentary study of the shelf of the Basque country. Journal of Marine Systems 72, 397-406.

Laborde, P., Urrutia, J., Valencia, V., 1999. Seasonal variability of primary production in the Cap-Ferret Canyon area (Bay of Biscay) during the ECOFER cruises. Deep-Sea Research II 46, 2057–2079.

Legeleux, F., Reyss J.-L., Etcheber H., Khripounoff A., 1996. Fluxes and balance of ^{210}Pb in the tropical northeast Atlantic. Deep-Sea Research I 43, 1321-1341.

Lončarić, N, van Iperen, J., Kroon, D., Brummer, G.-J.A., 2007. Seasonal export and sediment preservation of diatomaceous, foraminiferal and organic matter mass fluxes in a trophic gradient across the SE Atlantic. Progress in Oceanography 73, 27-59.

Mienert, J., Abrantes, F., Auffret, G., Evans, D., Kenyon, N., Kuijpers, A., Sejrup, H.P., van Weering, T.C.E., 1998. European North Atlantic Margin (ENAM I): sediment pathways, processes, and fluxes — an introduction. Marine Geology 152, 3-6.

Moore, W.S., Bruland, K.W., Michel J., 1981. Fluxes of uranium and thorium series isotopes in the Santa Barbara Basin. Earth and Planetary Science Letters 53, 391-399.

Muhammad, Z., Bentley, S.J., Febo, L.A., Droxler, A.W., Dickens, G.R., Peterson, L.C., Opdyke B.N., 2008. Excess ^{210}Pb inventories and fluxes along the continental slope and basins of the Gulf of Papua. Journal of Geophysical Research 113, doi:10.1029/2006JF000676.

Murphy, J., Riley, J.P., 1962. A modified single solution method for the determination of phosphate in natural waters. Analitica Chimica Acta 27, 31-36.

Ogawa, N., Tauzin, P., 1973. Contribution à l'étude hydrologique et géochimique du golfe de cap-breton. Bulletin de l'Institut Géeologique du Bassin d'Aquitaine, 19–46.

Oguri, K., Matsumoto, E., Yamada, M., Saito, 2003. Sediment accumulation rates and budgets of depositing particles of the East China Sea. Deep-Sea Research II 50, 513-528.

Radakovitch, O., Heussner, S., 1999. Fluxes and budget of ^{210}Pb on the continental margin of the Bay of Biscay (northeastern Atlantic). Deep-Sea Research II 46, 2175–2203.

Retailleau, S., Howa, H., Schiebel, R., Lombard F., Eynaud, F., Schmidt, S., Jorissen, F., Labeyrie, L., 2008. Planktic foraminiferal production along a depth transect in the southern Bay of Biscay. Continental Shelf Research, submitted.

Robbins, J., Edgington, D.N., 1975. Determination of recent sedimentation rates in Lake Michigan using ^{210}Pb and ^{137}Cs. Geochimica Cosmochimica Acta 39, 285-304.

Ruch, P., Mirmand, M., Jouanneau, J. -M., Latouche, C., 1993. Sediment budget and transfer of suspended sediment from the Gironde estuary to Cap Ferret Canyon. Marine Geology 111, 109-119.

Sanchez-Cabeza, J.A., Masqué, P., Ani-Ragolta, I., Merino, J., Frigani, M., Alvisi, F., Palanques, A., Puig, P., 1999. Sediment accumulation rates in the southern Barcelona continental margin (NW Mediterranean Sea) derived from ^{210}Pb and ^{137}Cs chronology. Progress in Oceanography 44, 313-332

Schmidt, S., 2006. Impact of the Mediterranean Outflow Water on particle dynamics in intermediate waters of the North-East Atlantic, as revealed by ^{234}Th and ^{228}Th. Marine Chemistry 100, 289-298.

Schmidt, S., Reyss, J.-L., 1996. Radium as internal tracer of Mediterranean Outflow Water. Journal of Geophysical Research 101, 3589-3596.

Schmidt, S., de Stigter, H.C., van Weering Tj.C.E., 2001. Enhanced short-term sediment deposition within the Nazare Canyon, North-East Atlantic. Marine Geology 173, 55-67.

Schmidt, S., van Weering, T.C.E., Reyss, J.-L., van Beek, P., 2002. Seasonal deposition and reworking at the sediment-water interface on the north-western Iberian Margin. Progress in Oceanography 52, 331-348.

Schmidt, S., Jouanneau, J-M., Weber, O., Lecroart, P., Radakovitch, O., Gilbert, F., Jezequel, D., 2007. Sedimentary processes in the Thau Lagoon (South France): from seasonal to century time scales. Estuarine Coastal Shelf Science 72, 534-542.

Schulz, H.D., Zabel, M., 2006. Physical properties of marine sediments. Marine Geochemistry, 2nd edition, Springer-Verlag Berlin Heidelberg, pp 27-71.

van Weering, Tj.C.E., Hall, I.R., de Stigter, H.C., McCave, I.N., Thomsen, L., 1998. Recent sediments, sediment accumulation and carbon burial at Goban Spur, N.W. European Continental Margin (47–50°N). Progress in Oceanography 42, 5-35.

van Weering, T.C.E., de Stigter, H.C., Boer, W., de Haas, H., 2002. Recent sediment transport and accumulation on the NW Iberian margin. Progress in Oceanography 52, 349-371.

Figure caption

Figure 1 - Map showing the sites of the sediment trap mooring (WH, star) and of interface cores (WH, A, B, D) on the slope of the Aquitanian margin (S.-E. Bay of Biscay).

Figure 2 – Profiles of $^{210}Pb_{xs}$ (dpm g^{-1}) and of porosity (g cm^{-3}) with depth in sediment.

Figure 3 - Time-series of total particulate mass flux trapped at 800 m and 1700 m respectively, and of sea surface temperature, estimated using remote sensing data, at the site WH.

Figure 4 - $^{210}Pb_{xs}$ activity (dpm g^{-1}), $^{210}Pb_{xs}$ flux (dpm m^{-2} d^{-1}) and organic carbon content (%) versus total mass flux (mg m^{-2} d^{-1}) at 800-m (left panel) and 1700-m (right panel). Both POC estimates are plotted (see main text for details): closed symbol: POC, open symbol: N-corrected POC.

Figure 5 - $^{210}Pb_{xs}$ activity (left panel) and F/P ratio (right panel) versus organic carbon content (%) for trapped particles at 800-m (dark triangles) and 1700-m (open triangles).

Figure 1

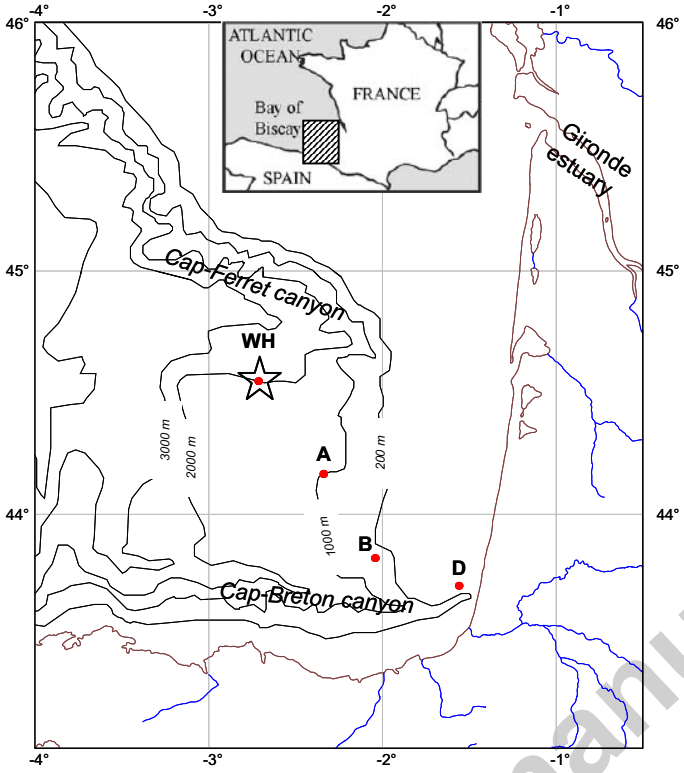

Figure 2

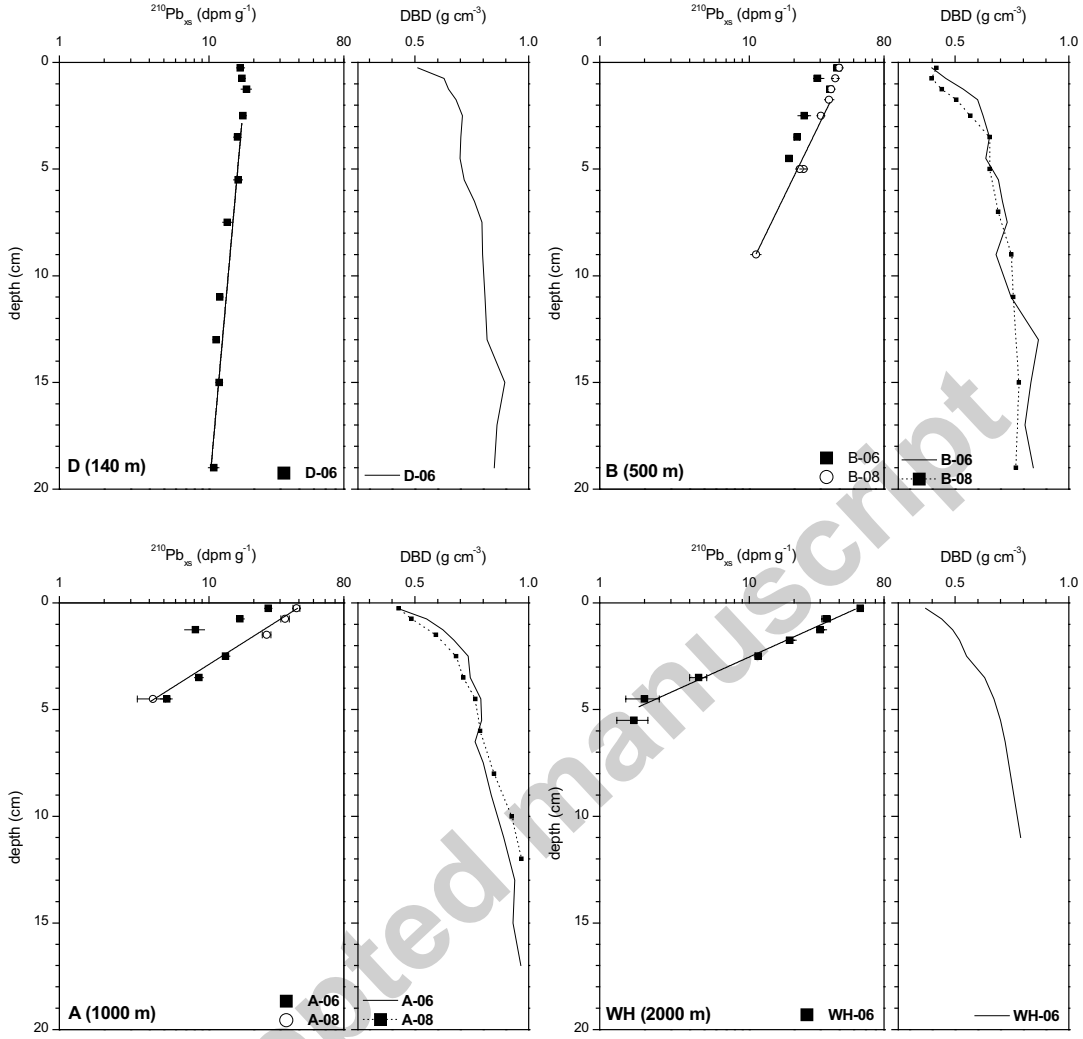

Figure 3

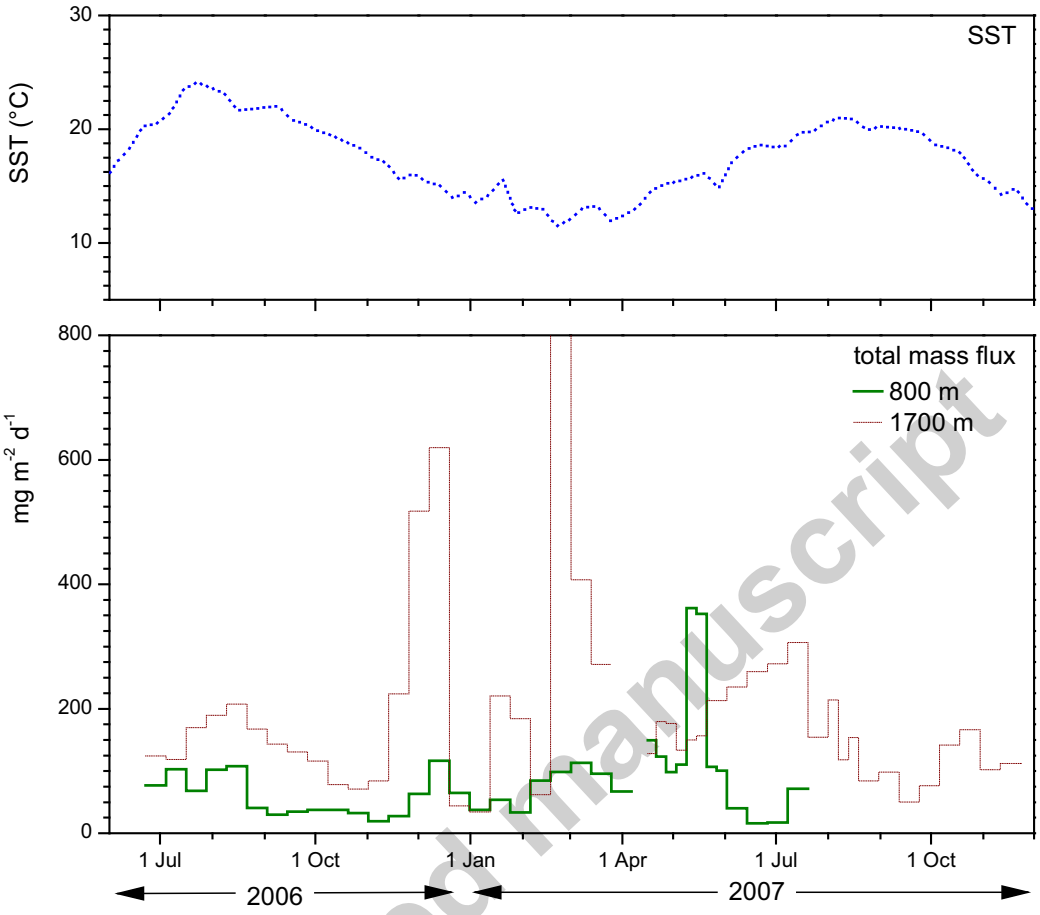

Figure 4.

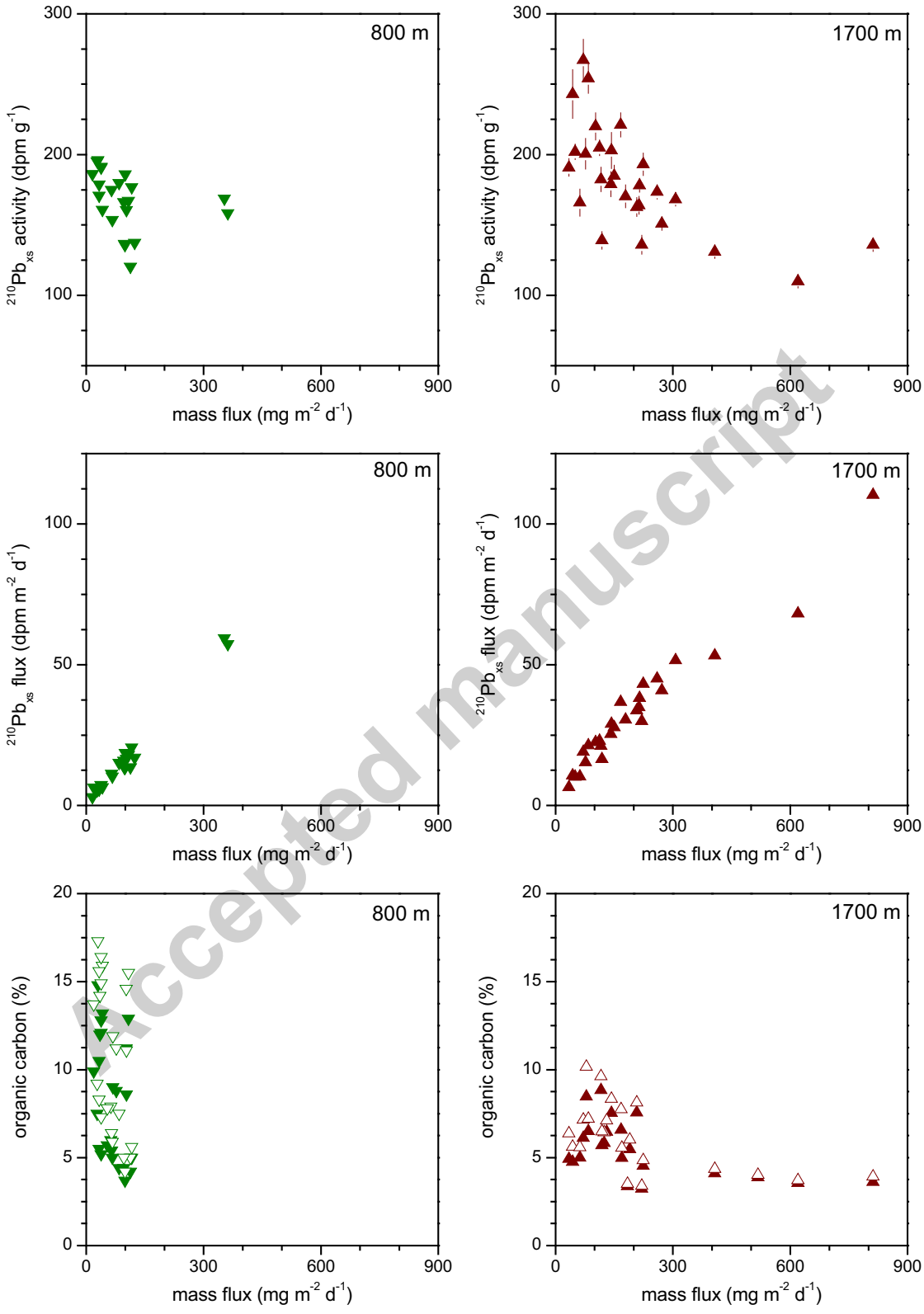

Figure 5.

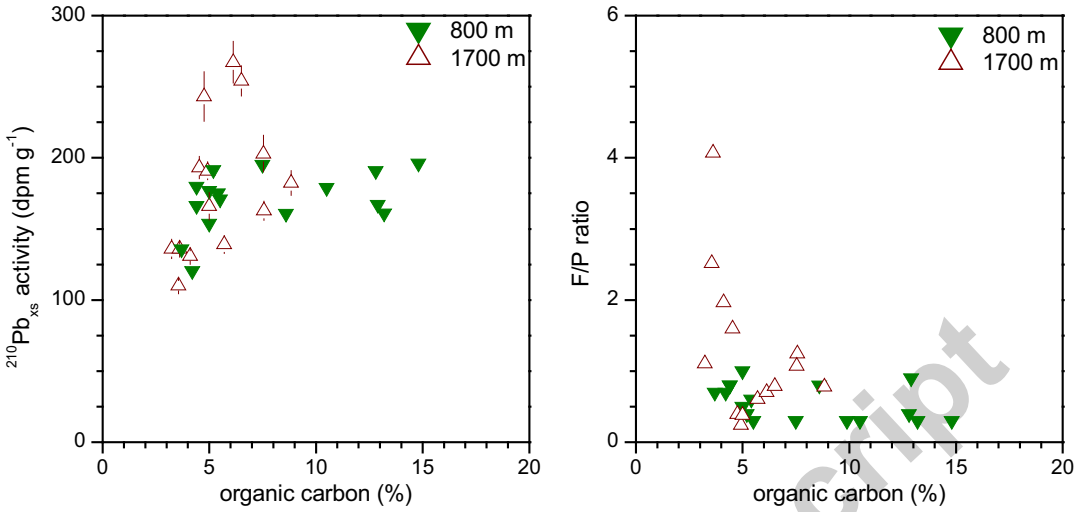

Table 1. Location, depth and sampling date of the cores, sediment and mass accumulation rates (SAR, MAR) derived from seabed $^{210}Pb_{xs}$ profiles and mean annual mass fluxes from traps. For core D, values are given just for comparison (see main text for details and figure 2).

Sites			**depth (m)**	**Sampling dates**	**Core**	**MAR (cm a^{-1})**	**SAR (mg cm^{-2} a^{-1})**	**mass flux (mg cm^{-2} a^{-1})**
D	43°42 'N	1°34' W	145	June, 2006	D-6	> 1.1	> 936	
B	43°50' N	2°03' W	550	June, 2006	B-06	0.12	95	
				April, 2008	B-08	0.22	156	
A	44°10' N	2°20' W	1000	June, 2006	A-06	0.05	69	
				April, 2008	A-08	0.06	42	
WH	44°33 N	2°45 W	800	June 2006 - Nov. 2007	*trap*			2.7
			1700	June 2006 - Nov. 2007	*trap*			7
			2000	June, 2006	WH-06	0.04	28	

Table 2. Dissolved ^{226}Ra distribution in the water column of site WH, ^{210}Pb production rate by ^{226}Ra at the depth of the considered trap or core, total ^{210}Pb production (P), ^{210P}b fluxes and ^{210}Pb flux/^{210}Pb annual production ratio (F/P). For trap, F/P values correspond to the weighted mean ratios, minimum and maximum values are indicated in bracket.

sites	**depth** (m)	**^{226}Ra** (10^{-2} dpm l^{-1})	**^{210}Pb production rate by ^{226}Ra decay** (dpm cm^{-2} a^{-1})	**Total ^{210}Pb production (P)** (dpm cm^{-2} a^{-1})		**^{210}Pb flux (F)** (dpm cm^{-2} a^{-1})	***F/P* ratio**
WH	75	9.2 ± 0.4					
	500	7.9 ± 0.4					
WH	800		0.21	0.72	trap	0.48	0.7 (0.2-3)
	1000	8.9 ± 0.4					
WH	1700	11.0 ± 0.7	0.48	0.99	trap	1.18	1.2 (0.2-4.1)
WH	2000		0.58	1.09	core	1.3	1.2
D	145		0.04	0.55	core	> 6.4	> 12
B	550		0.15	0.66	core	5.3 - 5.8	8.3-9.0
A	1000		0.26	0.77	core	1.4 - 1.6	1.8-2.1